Supplementary Material

Comparison of the cubic lattice parameters of monoolein/water and monoolein/octylglucoside/buffer-solution structures

Figure 1S shows the comparison of the thermal behavior of the Pn3m unit cell lattice parameter, *a*, of pure monoolein (MO) fully hydrated in water (filled triangles) with those of the presently investigated MO/OG (90/10, mol/mol) mixture hydrated in excess aqueous phase 0.1 M NaCl (phosphate buffer pH 7.0) (filled circles). The data for pure MO have been published in Czeslik C., Winter R., Rapp G., Bartels K., *Biophys.J.* **1995**, 68, 1423-1429. In excess water, the diamond type cubic lattice of pure MO transforms into a hexagonal phase at temperatures above 94 ^{o}C. Our dynamic X-ray scans established that the MO/OG cubic phase structure remains in the Pn3m space group symmetry up to 100 ^{o}C. The lattice spacing of the MO/OG cubic phase in buffer at 25 ^{o}C ($a_{(D_{Large})}$ = 15.1 nm) is by about 40% larger than that of pure MO in water ($a_{(D_{Normal})}$ = 10.7 nm) at same temperature.

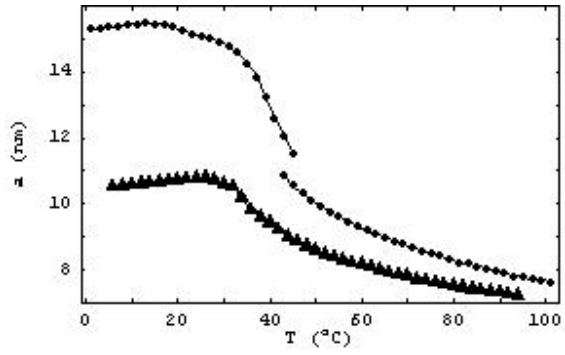

Figure 1S

Experimental synchrotron X-ray diffraction patterns of cubic MO/OG dispersions at selected temperatures and analysis of the X-ray reflections based on the GH model

Figure 2S shows experimental X-ray diffraction patterns of the investigated MO/OG mixture (90/10, mol/mol) at full hydration in 0.1 M NaCl phosphate buffer solution with pH 7. The presented frames were acquired at the indicated temperatures from a heating scan performed at a rate 2 ^{o}C/min from 1 to 100 ^{o}C. The scan rate was chosen after series of scans of MO/OG/water mixtures of various molar ratios. The investigated systems, including the one reported here, showed fast response to the temperature changes on heating.

The X-ray patterns recorded at temperatures 1 ^{o}C and 3 ^{o}C revealed that intensive reflections of a diamond type cubic lattice (space group Pn3m) overlap with low-intensity peaks of a primitive cubic lattice (space group Im3m). The green bars in Figure 2S index from left to right the positions of the maxima of the (110), (200), (211), (220), (310), (222), (321) and (400) reflections of an Im3m cubic lattice. The s-values of the peak maxima for Im3m cubic space group are spaced in the characteristic ratio $\sqrt{2} : \sqrt{4} : \sqrt{6} : \sqrt{8} : \sqrt{10} : \sqrt{12} : \sqrt{14} : \sqrt{16}$. The red bars in Figure 2S consecutively denote the (110), (111), (200), (211), (220), (221), and (310) reflections of a diamond cubic lattice. The X-ray peak set for a Pn3m cubic space group is identified by the characteristic ratio of the s-values of the diffraction maxima $\sqrt{2} : \sqrt{3} : \sqrt{4} : \sqrt{6} : \sqrt{8} : \sqrt{9} : \sqrt{10}$. The reflections of the primitive Im3m cubic phase vanished at temperatures above 5 ^{o}C.

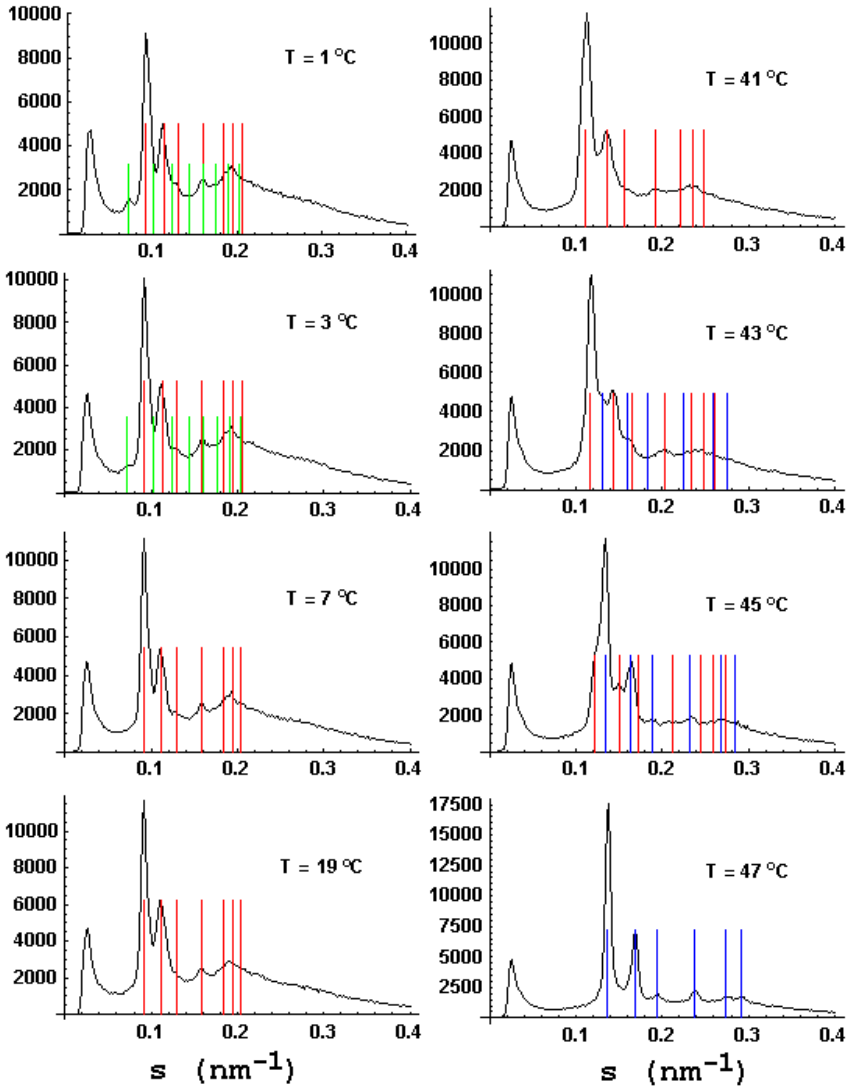

Figure 2S

The X-ray reflections recorded in the interval 5 °C < T < 100 °C were best fitted by a peak set typical for the diamond type cubic lattice (space group Pn3m). No other space group (from the presently known for cubic phases of hydrated amphiphiles) could better describe the experimentally observed X-ray diffraction peaks (Fig. 2S). Notably, a cubic-cubic structural transition was resolved to occur at temperature around 44 °C during the dynamic thermal scan. The positions of the Bragg peaks identifying the two diamond cubic lattices are indicated in Figure 2S by red (D_{Large}) and blue (D_{Normal}) bars, respectively.

A careful examination of the shape of the X-ray patterns at temperatures below 43 °C revealed remarkable differences with respect to the shape of the patterns at T > 45 °C. We established that at low temperatures the reflections of the diamond cubic lattice D_{Large}, characterized by a unit cell spacing around 15 nm, are superimposed on a large diffuse scattering with a maximum centered in the interval of spacings s~0.20÷0.25 nm^{-1} (see the green curves in Figures 3S and 4S at T= 19, 43 and 45 °C). At T < 43 °C, the diamond cubic phase, referred to as D_{Large} nonlamellar phase, displays Bragg peaks with larger widths and lower intensities as compared to the Bragg peaks resolved for the D_{Normal} cubic phase (Pn3m space group) at T > 45 °C.

During the heating scan, coexisting reflections of two diamond type cubic lattices were resolved at T = 43 ºC and T = 45 ºC (Figs. 2S and 4S). At T = 43 ºC, the peaks of the D_{Large} cubic phase (represented by red bars in Fig. 2S) are with stronger intensities as compared to those of the second cubic phase D_{Normal} (lower intensity peaks indexed in blue). At T = 45 ºC, the intensities of the peaks of the second diamond cubic phase (D_{Normal}) begin to increase, and at T > 47 ºC this nonlamellar phase is entirely dominating (see the peaks indexed by blue bars at T = 45 ºC and 47 ºC in Fig. 2S). Upon the growth of the D_{Normal} cubic phase, the intensity of the scattering background centered at s ~ 0.23 nm^{-1} diminishes by about 50% (see the green curve in Fig. 3S). At T > 45 ºC, the Bragg peaks of the D_{Normal} phase exhibited increased intensities and they were narrow in width. This indicates a longer-range correlation of the three-dimensional order at temperatures above the transition temperature 45 ºC.

Towards peaks fitting, the obtained diffraction patterns were normalized and the background was subtracted. Figures 3S and 4S show examples of the peak fitting. The red curves represent the Gaussian peak fitting for the D_{Large} cubic phase, the blue curves show the Gaussian peaks for the D_{Normal} cubic phase, and the green curves correspond to the diffuse scattering with maxima centered at s-spacings between 0.20 and 0.25 nm^{-1}.

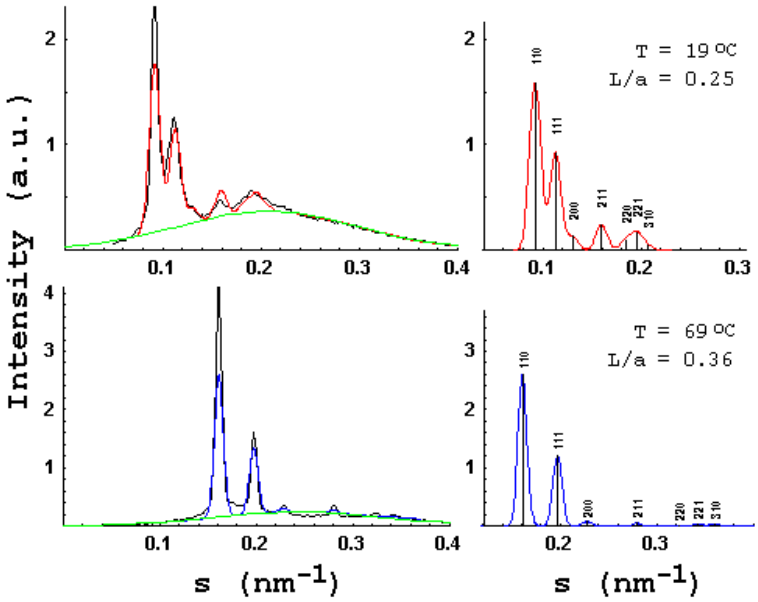

Figure 3S

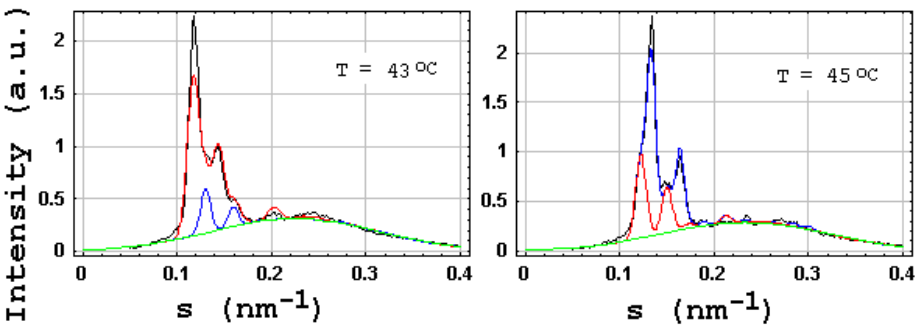

Figure 4S

Figure 3S presents the fitting of the X-ray patterns of the single diamond D_{Large} cubic phase at T = 19 °C (top red curves) and of the single diamond D_{Normal} cubic phase at T = 69 °C (bottom curves in blue). Figure 4S shows the peak fitting describing the cubic-cubic structural transition from D_{Large} to D_{Normal} phase. At 43 °C, the D_{Large} phase displays high-intensity reflections (red Gaussian peaks), while the D_{Normal} phase has been just nucleated upon the heating and displays low-intensity peaks (blue Gaussian curves). At 45 °C, the D_{Normal} peaks grow (blue Gaussian peaks), while the D_{Large} peaks vanish (red Gaussian peaks).

According to the theory of Gartecki and Hołyst[10] the relative intensities of the diffraction peaks for a given chemical composition depend on the thickness of the lipid bilayer, determining the distribution of the electron density in the 3D system. We determined the structural parameters of the diamond-type cubic lattices formed in fully hydrated MO/OG (90/10, mol/mol) mixture by a nonlinear regression. The lipid bilayer thickness, *L*, in the cubic lipid phase was estimated from the lattice parameter, a, on the basis of the GH model[10]. The intensities in the experimental X-ray patterns were fitted to model scattering intensities defined as

$$I_{hkl}^{(\mathrm{mod})}(\mathrm{L}) = M_{hkl}\left[F_{hkl}^{S*}\frac{\sin(\alpha_{hkl}\pi\left(h^2+k^2+l^2\right)^{1/2}L^*)}{\alpha_{hkl\ 2}\pi\left(h^2+k^2+l^2\right)^{1/2}}\right]^2 \qquad (1),$$

where $L^* = L/a$ is the dimensionless lipid layer thickness, F^{S*} is the dimensionless structure factor, M_{hkl} is a multiplicity factor, and α_{hkl} are correction parameters for particular cubic lattice types[10]. The shape of every reflection was modeled as a Gaussian peak with intensity calculated according to Eq. 1. For the practical realization, we used a multivariable nonlinear fitting procedure written as a Wolfram Mathematica notebook. The NonlinearRegress function from the package `NonlinearFit` was used (*Mathematica 3.0 Standard Add-on Packages*; Wolfram Research, Inc.; Cambridge University Press: Cambridge, 1996). It allowed us to perform an improved fitting.

Figure 3S clearly shows that the intensities of the (110), (111), (200), (211), (220), (221), and (310) reflections of the D_{Large} (L/a = 0.25) cubic lattice are not spaced in the same peak intensity ratio as those for the D_{Normal} (L/a = 0.36) cubic phase. The higher-order peaks of the D_{Normal} cubic phase appear to be with negligibly small intensities as compared to its first order reflection (110) (Fig. 3S). While preserving same indexing of the Bragg peaks in the D_{Large} and D_{Normal} patterns, the temperature-induce change in the sample chemical composition (reflecting the OG solubility in the MO matrix), as well as the associated changes in the lipid bilayer thickness and lipid hydration, causes an alteration of the electron density distribution in the nonlamellar 3D structure, which results in different relative peak intensities of the D_{Large} and D_{Normal} phases.

The results obtained for the lipid bilayer thickness, *L*, water channel thickness, D_W, and the cubic lattice parameters $a_{(D_{Large})}$ and $a_{(D_{Normal})}$ are given in Table 1S for selected temperatures (see the X-ray patterns in Figures 3S and 4S). D_W was calculated by the equation: $D_W = 0.707\ a - L$. The obtained bilayer thickness for the "normal" cubic phase is in accord with that for the pure MO. The established temperature dependence of the dimensionless bilayer thickness is smaller for the "normal" cubic lattice as compared to that for the "large" one. This feature probably results from the temperature variation of the cubic lattice constant, *a,* and the geometrical packing constraints of the two lipid monolayers in the bilayer. The diamond type cubic phase is the most stable bicontinuous amphiphilic cubic phase existing in excess water. This study demonstrated that it is capable of preserving a 3D nanoperiodicity of the cubic Pn3m space group in its swollen state in the presence of OG.

Table 1S

Temperature	**19 °C**	**43 °C**	**45 °C**	**69 °C**
$a_{(D_{Large})}$ [nm]	15.35	12.06	11.54	--
$a_{(D_{Normal})}$ [nm]	--	10.87	10.56	8.77
$L_{(D_{Large})}$ [nm]	3.84	3.6	3.44	--
$L_{(D_{Normal})}$ [nm]	--	3.99	3.92	3.2
D_W [nm] (D_{Large})	7.01	4.92	4.72	--
D_W [nm] (D_{Normal})	--	3.69	3.55	3.0